Dual Targeting of Arabidopsis HOLOCARBOXYLASE SYNTHETASE1: A Small Upstream Open Reading Frame Regulates Translation Initiation and Protein Targeting[1][W]

Juliette Puyaubert[2,3], Laurence Denis[2,4], and Claude Alban*

CNRS (UMR 5168)/CEA/Université Joseph Fourier/INRA (UMR 1200), CEA-Grenoble, Institut de Recherche en Technologies et Sciences pour le Vivant, Laboratoire de Physiologie Cellulaire Végétale, 38054 Grenoble cedex 9, France

Protein biotinylation is an original and very specific posttranslational modification, compartmented in plants, between mitochondria, plastids, and the cytosol. This reaction modifies and activates few carboxylases committed in key metabolisms and is catalyzed by holocarboxylase synthetase (HCS). The molecular bases of this complex compartmentalization and the relative function of each of the *HCS* genes, *HCS1* and *HCS2*, identified in Arabidopsis (*Arabidopsis thaliana*) are mainly unknown. Here, we showed by reverse genetics that the *HCS1* gene is essential for plant viability, whereas disruption of the *HCS2* gene in Arabidopsis does not lead to any obvious phenotype when plants are grown under standard conditions. These findings strongly suggest that HCS1 is the only protein responsible for HCS activity in Arabidopsis cells, including the cytosolic, mitochondrial, and plastidial compartments. A closer study of *HCS1* gene expression enabled us to propose an original mechanism to account for this multiplicity of localizations. Located in the *HCS1* messenger RNA 5′-untranslated region, an upstream open reading frame regulates the translation initiation of *HCS1* and the subsequent targeting of HCS1 protein. Moreover, an exquisitely precise alternative splicing of *HCS1* messenger RNA can regulate the presence and absence of this upstream open reading frame. The existence of these complex and interdependent mechanisms creates a rich molecular platform where different parameters and factors could control HCS targeting and hence biotin metabolism.

The compartmentalization of most pathways of plant primary metabolism is generally covered in physiology textbooks. Cell fractionation and immunohistochemical studies have revealed the extensive compartmentalization of plant metabolism. This compartmentalization and its associated regulations are crucial for the integrated understanding of plant metabolism and its adaptation to both developmental and environmental changes. However, the intracellular locations of the majority of proteins are still not known (Lunn, 2007) and the intricacy of different metabolisms and their regulation in the cellular context is still to be unraveled. Biotin (vitamin H) is a cofactor for some carboxylases and decarboxylases dealing with crucial metabolic processes such as fatty acid and carbohydrate metabolism (Knowles, 1989). The biotinylation of these enzymes is a posttranslational modification allowing the transformation of inactive apoproteins into their active *holo* forms. The covalent attachment of biotin is catalyzed by biotin protein ligase, also called holocarboxylase synthetase (HCS). D-Biotin is attached to a specific Lys residue of newly synthesized apoenzyme via an amide linkage between the biotin carboxyl group and a unique ε-amino-group of a Lys residue (Samols et al., 1988). It occurs in two steps as follows:

$$\text{D-biotin} + \text{ATP} \rightarrow \text{D-biotinyl-5′-AMP} + \text{PPi} \quad (1)$$

$$\text{D-biotinyl-5′-AMP} + \text{apocarboxylase} \rightarrow \text{holocarboxylase} + \text{AMP} \quad (2)$$

Biotin-dependent carboxylases are enzymes ubiquitously found in living cells. However, their number, structure, and subcellular localization are subject to variations according to organisms. In plants, four different biotin-dependent carboxylase activities have been evidenced: two structurally distinct isoforms of acetyl-CoA carboxylase (ACCase) in cytosol and plastids, geranoyl-CoA carboxylase in plastids, and methylcrotonoyl-CoA carboxylase (MCCase) in mitochondria (Alban et al., 2000). Moreover, sequencing of the Arabidopsis (*Arabidopsis thaliana*) genome confirmed the occurrence of genes encoding for both structural forms of ACCase and for MCCase (Nikolau et al.,

[1] This work was supported by the Ministère de l'Enseignement Supérieur et de la Recherche (fellowship to L.D.) and by INRA (postdoctoral fellowship to J.P.).

[2] These authors contributed equally to the article.

[3] Present address: Université Pierre et Marie Curie-Paris 6, CNRS UMR 7180, PCMP, F–94200 Ivry-sur-Seine, France.

[4] Present address: CNRS UMR 8541, Ecole Normale Supérieure, 46 rue d'Ulm, 75230 Paris cedex 05, France.

* Corresponding author; e-mail claude.alban@cea.fr.

The author responsible for distribution of materials integral to the findings presented in this article in accordance with the policy described in the Instructions for Authors (www.plantphysiol.org) is: Claude Alban (claude.alban@cea.fr).

[W] The online version of this article contains Web-only data.

www.plantphysiol.org/cgi/doi/10.1104/pp.107.111534

2003). As a result, plants offer a unique case of triple compartmentalization of biotin-dependent carboxylases. HCS activity localization in plant cell parallels this complexity. In pea (*Pisum sativum*) leaf cells, HCS activity was mainly located in cytosol of fractionated protoplasts, but a significant activity was also identified in both highly purified chloroplasts and mitochondria (Tissot et al., 1997). In Arabidopsis cultured cells, HCS activity was also essentially recovered in cytosol of fractionated protoplasts and, to a lesser extent, in the organelle subfraction (chloroplasts and/or mitochondria; Denis, 2002). This suggests that carboxylases are biotinylated in their compartment of residence.

The genetic and molecular bases of the compartmentalization of HCS activity are unclear. Two *HCS* genes have been evidenced in Arabidopsis (Tissot et al., 1997). Firstly, *HCS1* cDNA has been isolated by functional complementation of an *Escherichia coli* mutant (Tissot et al., 1997). Subsequently, the systematic sequencing of the Arabidopsis genome enabled the identification of the *HCS1* gene. Moreover, it confirmed the existence of a second *HCS* gene (*HCS2*) localized in the pericentromeric region of chromosome 1 (Arabidopsis Genome Initiative, 2000). *HCS1* and *HCS2* genes present very large similarities and probably result from the duplication of a common ancestor gene (Denis et al., 2002). The way both *HCS* genes share responsibility for in vivo HCS activity is unknown. A simple hypothesis would be that they present different substrate specificities or/and different subcellular localizations and cooperatively enable the biotinylation of the different carboxylase substrates. *HCS1* has been shown to encode a plastidial isoform of HCS and could then account for the chloroplastic HCS activity (Tissot et al., 1998). However, HCS1 presented a broad specificity of substrates and was able to biotinylate efficiently in vitro all recombinant biotin-dependent apocarboxylases identified in Arabidopsis (Tissot et al., 1998; Denis, 2002; Denis et al., 2002). Interestingly, *HCS2* expression produces a highly diverse family of alternatively spliced mRNAs (Denis et al., 2002). However, none of the putative HCS2 proteins, produced by alternative splicing of *HCS2*, was soluble and active in vitro when overproduced in *E. coli*, nor rescued an *E. coli* mutant affected in protein biotinylation (Denis, 2002). Also, western-blot analyses did not allow us to test the occurrence of these proteins in cellular extracts of Arabidopsis because HCS protein concentration in plant extracts was too low to be accurately detected (Denis et al., 2002). As a result, in vitro biochemical activity and substrate specificity alone did not give any definite evidence to partition the biotinylation of carboxylase proteins between HCS1 and HCS2. In this study, we report the isolation and characterization of *hcs1* and *hcs2* Arabidopsis mutants. From the result of our genetic and molecular analyses, we suggest that *HCS1* is the only *HCS* gene responsible for the biotinylation of all carboxylases in plants. Closer scrutiny of *HCS1* gene expression and splicing led us to revisit the specific compartmentalization of HCS1 proteins. We show that the *HCS1* mRNA 5′-untranslated region (UTR) is subjected to alternative splicing that affects the translation initiation at two AUG codons, enabling dual localization of HCS1 protein in cytosol and chloroplasts.

RESULTS

HCS1 and *HCS2* Are Neither Redundant Nor Cooperative to Mediate Carboxylase Biotinylation in Plants

Various collections of T-DNA and transposon insertion mutants were searched for disruption in *HCS1* and *HCS2* genes. We identified a line of Arabidopsis plants (SAIL_1277_E03; line *hcs1-1*) carrying an inverted tandem insert of T-DNA with a Basta resistance marker within the second exon of the *HCS1* gene (*At2g25710*; Fig. 1A). Segregating plants originating from the mutant line were genotyped by PCR using primers specific of the *HCS1* gene and of the T-DNA left border (Fig. 1B). This PCR analysis did not reveal any lines presenting a homozygous disruption of the *HCS1* gene. Moreover, self-pollination of heterozygous plants for the T-DNA insertion produced, in the next generation, wild-type and heterozygous plants at a ratio close to 1:1. Among a total of 95 progeny plants examined, no plants homozygous for the T-DNA insertion were recovered. Basta resistance segregation indicated that no additional T-DNA was inserted elsewhere in the genome. Indeed, all wild-type plants were Basta sensitive and all heterozygous plants were Basta resistant. These segregation data suggest that transmission of the inserted allele might be impaired in either the female or male gametes (or both), consistent with a gametophytic defect. The examination of immature siliques of self-pollinated heterozygous plants confirmed this hypothesis. They were found to contain approximately 60% normal-sized seeds, 30% to 40% empty slots filled with apparently aborted ovules that had not been fertilized, and aborted embryos at a reduced frequency (<10%; Fig. 1, C and D). Given that homozygous mutant plants were never recovered, we assume that aborted seeds corresponded to missing homozygous mutants. Aborted ovules suggest a defect of female gametogenesis. This was examined by back crossing of mutant plants. If the mutation is borne by the female parent (heterozygous mutant female flower crossed with wild-type pollen), the resulting siliques contained roughly one-half the number of seeds per silique as the wild-type siliques. Of the plants grown from 30 of these seeds, 25 of them were found to be of the wild-type genotype and the other five were of the heterozygous genotype, based on PCR genotyping and Basta selection. If the mutation was borne by the male parent (wild-type mutant female flower crossed with heterozygous pollen), the resulting siliques contained the same number of seeds per silique as the wild-type siliques. One-half of them had the

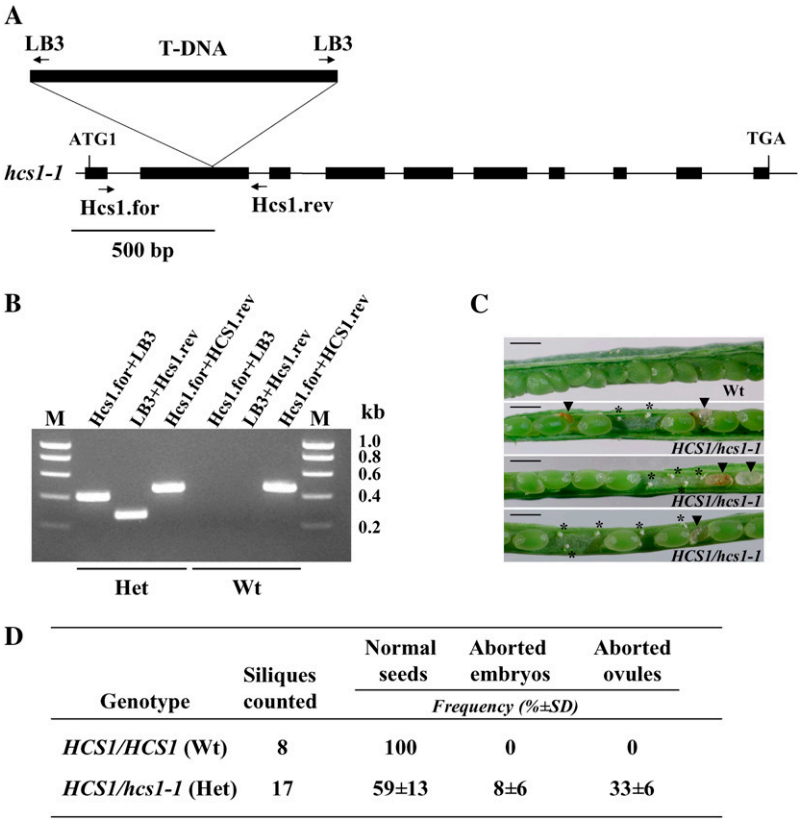

D

Genotype	Siliques counted	Normal seeds	Aborted embryos	Aborted ovules
		Frequency (%±SD)		
***HCS1/HCS1* (Wt)**	8	100	0	0
***HCS1/hcs1-1* (Het)**	17	59±13	8±6	33±6

Figure 1. Characterization of a T-DNA insertion allele of Arabidopsis *HCS1* (SAIL_1277_E03; line *hcs1-1*). A, Structure of the *HCS1* gene carrying the inverted tandem insert of T-DNA. Black boxes and lines indicate exons and introns, respectively. The size of T-DNA is not drawn to scale. The locations of primer sequences used for PCR genotyping are marked with arrows. B, Characterization of the T-DNA insertion locus by PCR. Genomic DNA from a wild-type (Wt) and a heterozygous *HCS1/hcs1-1* mutant (Het) plant was amplified using the primer combinations indicated. Three PCR reactions per plant were performed. HCS1.for and Hcs1.rev amplify a 0.46-kb product from the wild-type allele, LB3 and Hcs1.rev amplify a 0.29-kb product from the disrupted allele, and Hcs1.for and LB3 amplify a 0.41-kb product from the disrupted allele. Left and right flanking lanes (M) show DNA size markers. C, Light microscopy analysis of a wild-type immature silique showing uniform seed development and heterozygous *HCS1/hcs1-1* immature siliques containing aborted, white, and shrunken ovules (asterisks) and aborted, white or brown, and shriveled seeds (arrowheads). Scale bars = 500 μm. D, Seed production from wild-type (*HCS1/HCS1*) and heterozygous (*HCS1/hcs1-1*) Arabidopsis plants. Three types of seed/ovules were identified in the siliques and counted: normal seeds containing full-size embryos, abnormal seeds containing aborted embryos, and aborted white ovules.

wild-type genotype and one-half had the heterozygous genotype (from 30 plants, analyzed by PCR and Basta resistance). As a result, genetic crossing data support the notion that *HCS1* disruption causes ovule lethality. In summary, our results reveal that insertion in the *HCS1* gene is lethal, resulting in decreased transmission through the female gametophyte and homozygous embryonic lethality. Examination of a second independent *hcs1* disruption allele (FLAG_486E08; line *hcs1-2* obtained from the Versailles collection) presenting a single T-DNA insertion within intron 9 confirmed that the ovule and embryo abortions were caused by the T-DNA insertions into *HCS1* gene (see Supplemental Fig. S1).

To obtain an Arabidopsis *hcs2* knockout mutant, we screened a T-DNA insertion population (Bouchez et al., 1993) by PCR analysis of DNA pools with specific sets of primers derived from the *HCS2* gene and the T-DNA and molecular hybridization. One candidate knockout line (line 21) was obtained, and the location of the T-DNA insertion was determined by DNA sequence analysis of the PCR product. As shown in Figure 2A, the T-DNA was found to be inserted in intron 9 of the *HCS2* gene, 5 bp upstream of the beginning of exon 10. The line 21 presented a single T-DNA insertion (shown by the segregation of the kanamycin resistance in the F_2 progeny and Southern-blot analysis). Plants (T_3 generation) were examined by PCR. Among this population, wild-type plants as well as homozygous and heterozygous siblings were identified (Fig. 2B). As a result, the homozygous disruption of *HCS2* is not lethal. Wild-type and homozygous plants for the insertion were then self-pollinated for further molecular and biochemical analyses. To assess the impact of T-DNA insertion on gene expression, real-time quantitative reverse transcription (RT)-PCR was performed on mRNA from aerial plant sections comprising rosette leaves, stems, inflorescence, and developing siliques (Fig. 2C). The *HCS2* mRNA level in the plants homozygous for the T-DNA insertion did not exceed the background noise of PCR, while wild-type levels of *HCS2* transcripts were found in heterozygous plants. Interestingly, expression of *HCS1* gene was not altered in the *hcs2* null mutant, indicating that abolition of *HCS2* gene expression was not compensated by an overexpression of the *HCS1* gene, at least at the transcriptional level. The phenotype of the homozygous *hcs2* knockout mutant was carefully inspected, compared with the wild type, under standard greenhouse growth conditions. No detectable difference was observed at any growth stage, including seed germination, plant morphology and growth, seed production, and fertility (data not shown). To determine HCS2's part in biotinylation of biotin-dependent carboxylases, we first measured total HCS activity in soluble plant protein extracts using different Arabidopsis apocarboxylase substrates (recombinant proteins produced in *E. coli*). Surprisingly, protein extracts

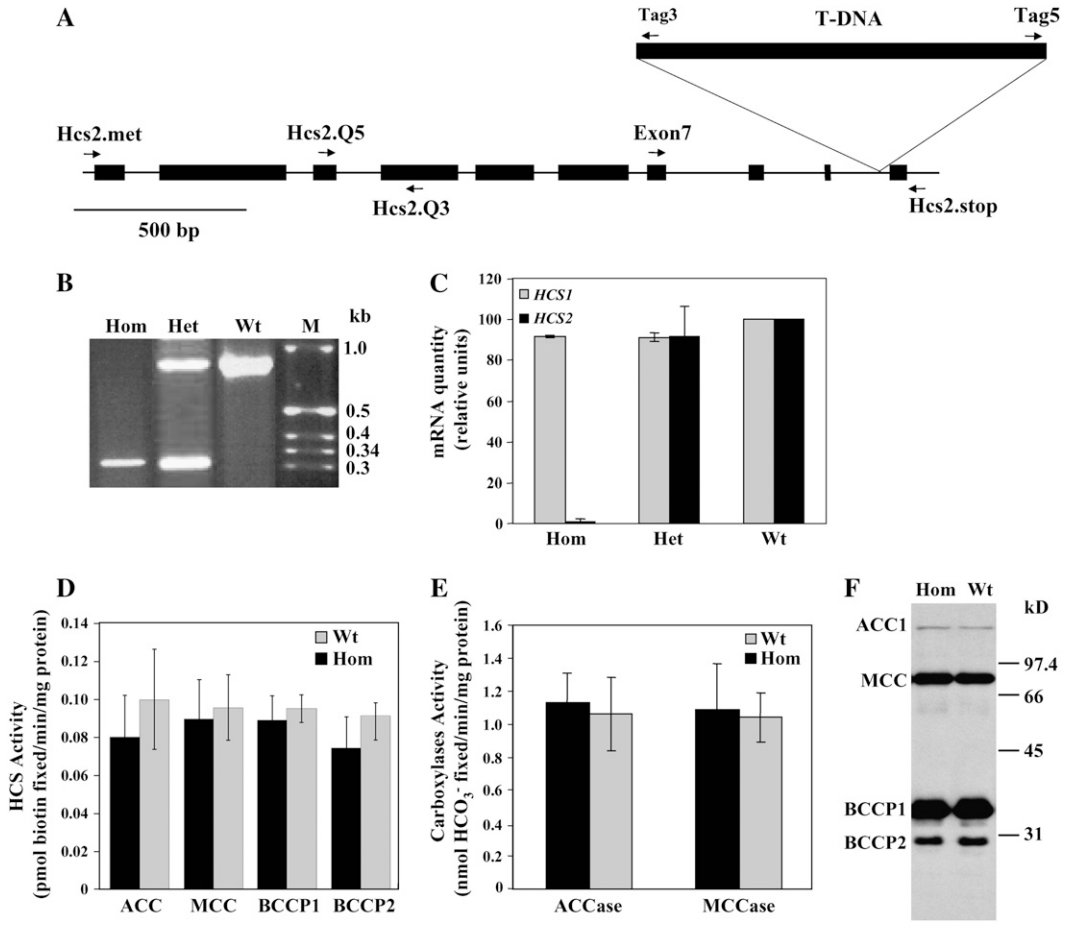

Figure 2. Identification and characterization of a T-DNA insertion allele of Arabidopsis *HCS2*. A, Structure of the *HCS2* gene carrying the T-DNA insertion. Black boxes and lines indicate exons and introns, respectively. The size of T-DNA is not drawn to scale. The locations of primer sequences used for molecular analyses (screening of the T-DNA insertion lines collection, PCR genotyping, and mRNA quantification) are marked with arrows. B, Characterization of the T-DNA insertion locus by PCR. Genomic DNA from a wild-type (Wt), a heterozygous *HCS2/hcs2* mutant (Het) plant, and a homozygous *hcs2/hcs2* mutant (Hom) plant was amplified using primers Exon 7, Hcs2.stop, and Tag5. Exon 7 and Hcs2.stop amplify a 0.84-kb product from the wild-type allele, and Tag5 and Hcs2.stop amplify a 0.32-kb product from the disrupted allele. C, Real-time RT-PCR quantification of *HCS1* and *HCS2* gene expression in the wild-type (Wt), heterozygous (Het), and homozygous (Hom) mutant plants. The relative amount of *HCS1* and *HCS2* mRNAs in aerial parts of Arabidopsis plants was determined using specific primers (Table I) as described in ''Materials and Methods.'' Data (relative transcripts abundance normalized to the expression levels in wild-type plants) are means of three independent experiments performed with three cDNA dilutions ± SD. *ACTIN1* was used as an internal control to normalize for variation in the amount of cDNA template. D, HCS activity measurements in protein extracts from wild-type (Wt) and homozygous (Hom) mutant plants using recombinant ACC138 (ACC), MCC220 (MCC), BCCP1, and BCCP2 as the apocarboxylase substrates. Data are means ± SD of four independent determinations. E, ACCase and MCCase activity measurements in protein extracts from wild-type (Wt) and homozygous (Hom) mutant plants. Data are means ± SD of three independent determinations. F, Western-blot analysis of biotinylated proteins in protein extracts from wild-type (Wt) and homozygous (Hom) mutant plant leaves using streptavidin coupled to peroxidase for detection. Each fraction contained 50 μg proteins. ACC1, MCCα, BCCP1, and BCCP2 proteins are indicated to the left. Position of molecular mass markers is given on the right.

from *hcs2* mutant plants presented wild-type levels of HCS activities, in vitro, irrespectively of the apocarboxylase substrate used in the reaction (Fig. 2D). Western-blot analyses of biotinylated proteins using streptavidin coupled to peroxidase showed that the absence of HCS2 expression does not affect the biotinylation of biotin-dependent carboxylases in planta (Fig. 2F). In the same protein extract, biotin-dependent carboxylase (MCCase and ACCase) activities were found to be similar in both mutant and wild-type lines (Fig. 2E). This confirms that in planta protein biotinylation was not affected by *HCS2* disruption.

Altogether, our results support the idea that the *HCS2* gene has no or limited implication in biotin-dependent carboxylase biotinylation in planta, and that the *HCS1* gene is responsible for most, if not all, plant HCS activity and as such is essential for plant viability. Therefore, *HCS1* and *HCS2* are not functionally redundant

and they do not share the activity of biotinylation of different carboxylases in planta. How could *HCS1* be responsible for the different HCS activities evidenced in different compartments of the plant cell?

The 5′-UTR of *HCS1* mRNA Is Subjected to Alternative Splicing

Functional complementation of an *E. coli* mutant enabled us to identify one mRNA variant of *HCS1* (Tissot et al., 1997). It encodes an in vitro active form of HCS and was thought to be the only mRNA transcribed from the *HCS1* gene. However, 5′-RACE experiments evidenced two populations of *HCS1* mRNA (Denis et al., 2002), *HCS1.s* (for spliced) and *HCS1.un* (for unspliced), generated by alternative splicing of the same *HCS1* pre-mRNA (Fig. 3). *HCS1.un* sequence was identical to the previously identified cDNA sequence. However, in the 5′-UTR of *HCS1.s* mRNA, 101 nucleotides are spliced out. A closer analysis of *HCS1.un* cDNA sequence enabled us to evidence a small open reading frame (ORF) of 24 nucleotides length (including the stop codon) located four bases upstream of the first ATG codon (Fig. 3). In *HCS1.s* mRNA, this sequence is spliced out, the stop codon of the 24-nucleotide small ORF coinciding with the 3′ acceptor signal.

Such elements, referred to as upstream ORF (uORF), are often found in the 5′-UTR of eukaryotic mRNA, yeast and fungi (McCarthy, 1998; Vilela and McCarthy, 2003), plants (Hanfrey et al., 2003), and mammals (Vattem and Wek, 2004). uORF can regulate the downstream ORF encoding the major gene product (Morris and Geballe, 2000; Meijer and Thomas, 2002). *HCS1* mRNA offers two in-frame AUG (AUG_1 and AUG_2), possibly representing initiation codons (Tissot et al., 1997). The amino acid sequence encoded by the region located between AUG_1 and AUG_2 corresponds to the cleavable transit peptide, targeting the longest form of HCS1 into chloroplasts (Tissot et al., 1998). Initiation at AUG_1 or AUG_2 could then produce HCS proteins with different subcellular localizations. The double occurrence of an alternatively spliced uORF (now referred to as uORF24) and two possible AUG start codons in the 5′-end of the *HCS1* main ORF offers a good environment for a possible translational control. This interesting observation led us to investigate the influence of uORF24 on translation initiation at AUG_1 and AUG_2.

uORF24 Controls in Vitro Translation of the Downstream *HCS1* Main ORF

To determine the influence of the uORF on translation initiation, we studied translation of both *HCS1* mRNA species by in vitro transcription-translation of full-length cDNA variants, isolated by RT-PCR, and subcloned in pPCRscript (Fig. 4A). In vitro transcription-translation of *HCS1.un* cDNA produced a major peptide of 37 kD corresponding to the translation beginning at AUG_2. As a result, translation at AUG_1 is impeded when it is preceded by the full-length *HCS1* 5′-UTR. The *HCS1.s* mRNA translation profile was quantitatively and qualitatively different. The amount of HCS1

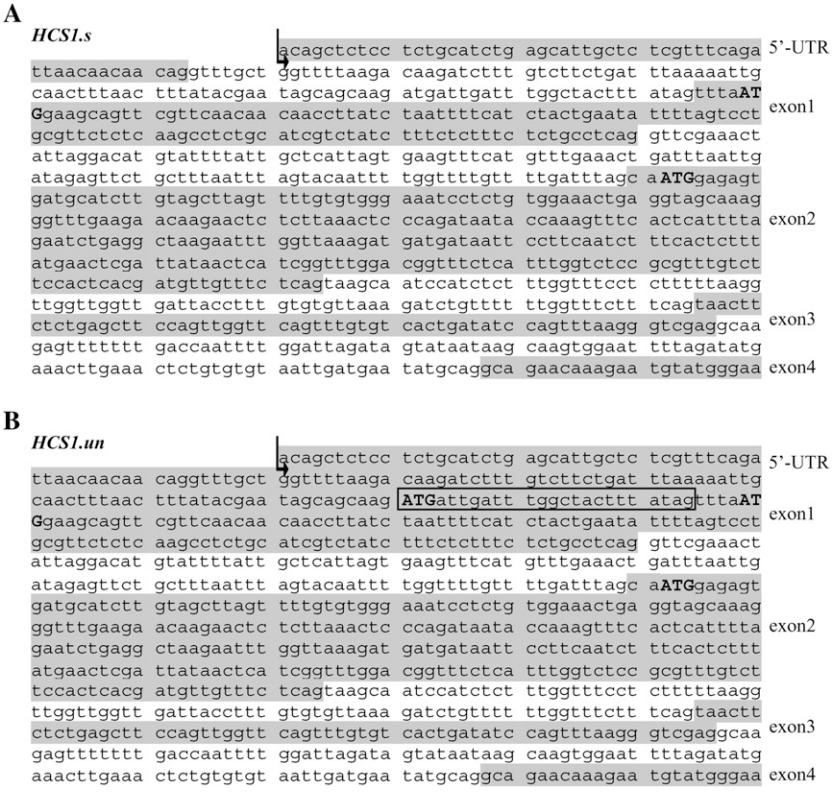

Figure 3. The 5′ upstream region of Arabidopsis *HCS1.un* and *HCS1.s* cDNA species. The 5′ sequence of the *HCS1* gene (*At2g25710*) is reported. Sequences of cDNAs obtained by RACE or RT-PCR are shaded. Initiation codons are in uppercase letters and in bold. Arrows indicate the experimentally obtained transcription start site (Denis et al., 2002). A, Nucleotide sequence of the 5′-UTR and of the first four exons of the *HCS1* cDNA spliced isoform. B, Nucleotide sequence of the 5′-UTR and of the first four exons of the *HCS1* cDNA unspliced isoform. The uORF is boxed.

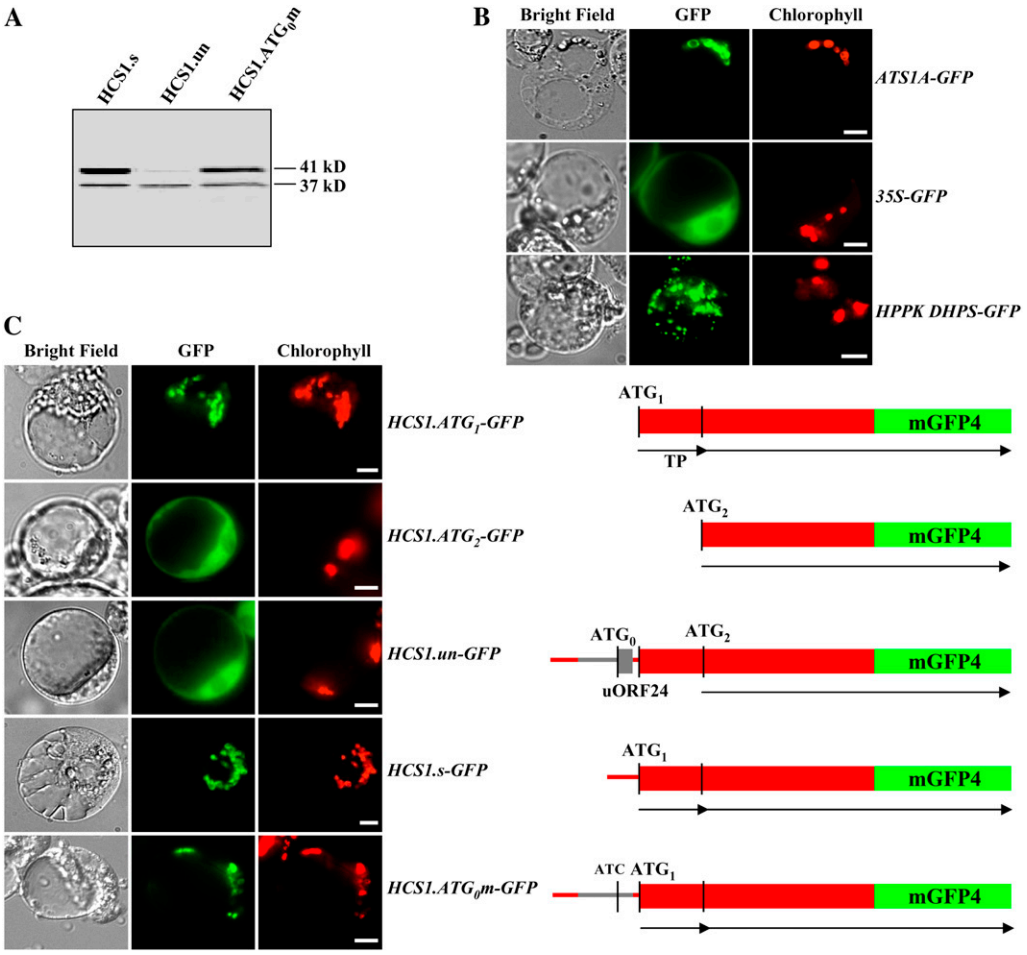

Figure 4. The nature of the 5′-UTR of *HCS1* mRNA influences AUG choice in vitro and controls the targeting of HCS1 protein in vivo. A, In vitro transcription-translation experiments. Polypeptides radioactively labeled with [^{35}S]Met were subjected to SDS-PAGE and analyzed by phosphorimaging as described in "Materials and Methods." Fluorography of translation products obtained with 1 μg of pPCRscript-HCS1.s (lane 1), 1 μg of pPCRscript-HCS1.un (lane 2), and 1 μg of pPCRscript-HCS1.ATG$_0$m (lane 3). The apparent molecular masses of the polypeptides produced are indicated on the right. B and C, Transient expression of GFP-fusion proteins in Arabidopsis protoplasts. B, GFP alone (35S-GFP) and chimera between GFP and the transit peptides of the small subunit of Rubisco (ATS1A-GFP) or dihydropterin pyrophosphokinase/dihydropteroate synthase (HPPK DHPS-GFP) were used as controls for the targeting of the reporter protein to the cytosol, chloroplasts, and mitochondria, respectively. C, Various plasmid constructs engineered with *HCS1* cDNA sequences fused upstream and in frame with GFP sequence were introduced into Arabidopsis protoplasts as described in "Materials and Methods." Schematic representations of cDNA constructs used are shown on the right of corresponding images. TP, Transit peptide. Images are optical photomicrographs (bright field), GFP fluorescence (GFP; green pseudocolor), and chlorophyll fluorescence (chlorophyll; red pseudocolor). Scale bars = 10 μm.

protein synthesized is increased when *HCS1.s* is translated as compared to *HCS1.un*. Therefore, the 5′-UTR sequence, spliced out in *HCS1.s* and retained in *HCS1.un*, has an inhibitory effect on HCS1 translation. Moreover, even if the translation of *HCS1.s* produced the same 37-kD polypeptide as *HCS1.un*, it was not the major translated product. A more abundant 41-kD protein was also synthesized, from the initiation of translation at AUG$_1$. These results suggested that the 5′-UTR of *HCS1* mRNA can influence the choice between AUG$_1$ and AUG$_2$. Can these results be explained by the presence (in *HCS1.un*) or absence (in *HCS1.s*) of uORF24? To understand uORF24 influence on *HCS1* translation initiation, we performed site-directed mutagenesis. uORF24 initiation codon (ATG$_0$) was changed to ATC codon in *HCS1.un* cDNA and the mutant analyzed by in vitro transcription and translation. The mutated *HCS1.un* cDNA presented the same pattern as *HCS1.s* and can produce a 41-kD protein in large abundance. This suggests that the modification of translation efficiency and AUG choice associated with the splicing of 5′-UTR of *HCS1* is directly dependent on the presence or absence of uORF24 itself and not on some structural changes possibly produced by the splicing removal of 101 nucleotides. In the presence of the uORF24 within the 5′-UTR of *HCS1* mRNA (*HCS1.un*), translation initiates mainly at AUG$_2$. In its absence, either due to elimination by alternative splic-

ing of the *HCS1* pre-mRNA (*HCS1.s*) or by mutation of AUG_0 codon (*HCS1.ATG$_0$m*), translation initiates predominantly at AUG_1, yielding the longer HCS1 form.

In Vivo uORF24 Controls the Targeting of HCS1 Protein

To follow the consequences of *HCS1* 5′-UTR splicing in vivo, we designed reporter plasmids bearing spliced or unspliced *HCS1* 5′-UTR tagged on the sequence coding the first 142 residues of *HCS1* main ORF in frame with GFP coding sequence. These constructs, along with different control constructs, were transiently expressed into Arabidopsis protoplasts, and the resulting GFP fluorescence (reporting HCS1 expression and localization) was analyzed (Fig. 4, B and C). As expected, the expression in protoplasts of the control construct *35S:HCS1.ATG$_1$-GFP* (translation starting at AUG_1) marked the plastids with GFP fluorescence (colocalized with the red autofluorescence of chlorophyll). This result was in good agreement with a previous immunocytological study showing that tobacco plants stably transformed with the Arabidopsis *HCS1* cDNA coding sequence driven by the cauliflower mosaic virus 35S promoter accumulated recombinant HCS1 protein within chloroplasts (Tissot et al., 1998). On the other hand, the control construct *35S:HCS1.ATG$_2$-GFP* (translation starting at AUG_2) expression led to a diffuse cytosolic GFP fluorescence. Arabidopsis protoplasts transfected with *35S:HCS1.un-GFP* construct exhibited GFP fluorescence spread throughout the cytosol. This suggests that, in vivo, an unspliced 5′-UTR favors the utilization of AUG_2, which, by eluding the transit peptide, leads to a cytosolic localization. In contrast, the expression of *35S:HCS1.s-GFP* construct resulted in a pattern of GFP fluorescence corresponding to the plastid pattern observed after transfection of protoplasts with p35S:HCS1.ATG$_1$-GFP control plasmid. This suggests that splicing of *HCS1* 5′-UTR abrogates in vivo the inhibition of AUG_1 initiation and enables the synthesis of a longer HCS1 precursor form and its plastidial targeting. Finally, mutagenesis of ATG_0 codon in *HCS1un-GFP* (*35S:HCS1.ATG$_0$m-GFP*) restored the plastidial fluorescence localization associated with the expression of *HCS1s-GFP*. This confirms that uORF24 itself (and not a global structure of *HCS1* 5′-UTR) controls the initiation of translation in vivo and the subsequent targeting of HCS1 protein.

Both in vivo and in vitro, our data demonstrate that alternative splicing of the 5′-UTR of *HCS1* mRNA controls the dual targeting of HCS1 protein through alternative use of distinct initiation codons and that uORF24 is essential for the AUG choice. The presence of uORF24 within the 5′-UTR of *HCS1* cDNA (*HCS1.un*) precludes AUG_1 utilization and favors the synthesis of a short protein form initiated at AUG_2, which consequently localizes in the cytosol. In the absence of uORF24 (*HCS1.s* or *HCS1.ATG$_0$m*), the translation initiation begins at AUG_1, allowing the production of a HCS1 protein headed by a transit peptide.

HCS1.un and *HCS1.s* Are Expressed in Every Organ of Arabidopsis, But the Former That Encodes a Cytosolic HCS1 Protein Is Predominant

The model previously presented was drawn from the results of RACE and RT-PCR experiments, and the subsequent molecular and functional analysis of the two resulting cDNA products. To test the significance and relevance of this model, we sought to check the presence of *HCS1.un* and *HCS1.s* transcripts in planta. We also investigated the cellular distribution of HCS1 protein by means of subcellular fractionation studies.

By means of quantitative RT-PCR measurements, we evaluated *HCS1.un* and *HCS1.s* transcript relative abundance in various plant organs (Fig. 5). *HCS1.un* and *HCS1.s* mRNA were detected in all analyzed organs (roots, stem, leaves, green siliques, flowers, and mature seeds). This evidenced the ubiquitous existence of an alternative splicing of *HCS1* and validated the significance of our model. Moreover, in all plant organs tested, the relative amount of *HCS1.un* mRNA was much greater (about 50- to 200-fold higher) than *HCS1.s* mRNA. This last observation was in good agreement with previous findings showing that HCS activity is mostly present (up to 90% of total activity) in cytosol of plant cells (Tissot et al., 1997; Denis, 2002), *HCS1.un* transcript encoding a cytosolic HCS1 form. In addition, we showed by in vitro translation experiments that *HCS1.s* is more efficiently translated than *HCS1.un*. The maintenance of a large pool of unspliced *HCS1* mRNA could then, at the same time, assure that a large majority of HCS1 protein is targeted to the cytosol and enable, upon its splicing, a rapid and efficient synthesis of plastidial HCS1 protein.

As a complementary approach, we investigated the subcellular distribution of HCS1 in Arabidopsis by western blot. Importantly, under our assay conditions, affinity-purified HCS1 antibody used in this study was specific to HCS1 proteins and did not cross react with recombinant HCS2 (Fig. 6A). Intact chloroplasts and mitochondria from Arabidopsis leaves were purified on Percoll density gradients, thus providing organelles devoid of contamination from the other compartments (Fig. 6B). Also, a cytosolic-enriched fraction was prepared. Soluble proteins from purified chloroplasts, mitochondria, and the cytosolic-enriched fractions were then analyzed. To overcome the difficulty in immunodetection of the endogenous protein due to its low abundance, we used a sensitive chemifluorescent system for detection. As expected, antibodies raised against recombinant HCS1 protein identified HCS1 mainly in the cytosol (Fig. 6A). The apparent molecular mass of the detected polypeptide was identical to that of recombinant HCS1-ATG$_2$, in good agreement with an initiation of translation at AUG_2 codon for cytosolic HCS1. Moreover, a polypeptide of the expected size for mature HCS1 (a transit peptide cleavage site is predicted in the HCS1-ATG$_1$ sequence one amino acid upstream the AUG_2 encoded Met residue; Tissot et al., 1998) was also detected in chloroplasts and in mito-

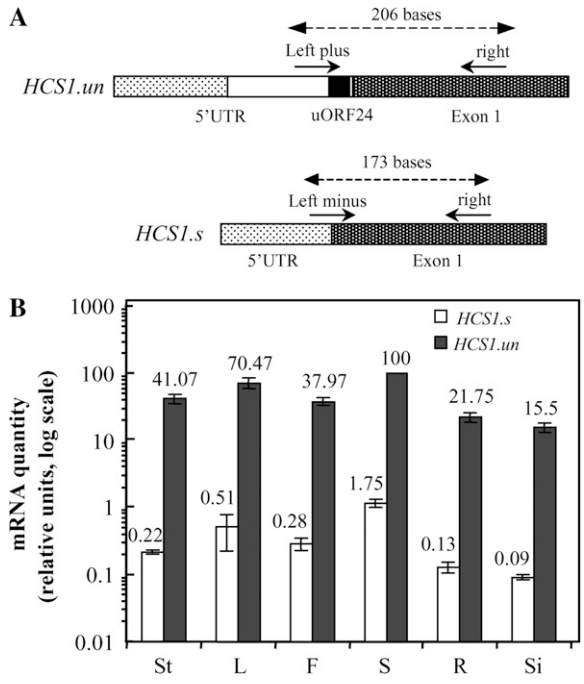

Figure 5. Relative abundance of *HCS1.s* and *HCS1.un* mRNA species in Arabidopsis organs. A, Schematic representation of left plus, left minus, and right oligonucleotide positions on *HCS1* cDNA variants. Left plus oligonucleotide enabled the quantification of *HCS1.un* mRNA. Left minus oligonucleotide enabled the quantification of *HCS1.s* mRNA. B, Real-time RT-PCR experiment on poly(A^+) RNA from various Arabidopsis organs (roots [R], stems [St], leaves [L], flowers [F], siliques [Si], and seeds [S]) using *HCS1.s*- and *HCS1.un*-specific primers. Data (relative transcripts abundance normalized to the expression level of *HCS1.un* in seeds) are means of three independent experiments performed with three cDNA dilutions ± SD. *ACTIN1* was used as an internal control to normalize for variation in the amount of cDNA template. Note the log scale in *y* axis.

chondria, albeit to a lower proportion. This labeling pattern correlated well with HCS specific activity measured in the same fractions.

Taken together, these results suggest that the model deducted from our molecular analysis is relevant and most probably presents an important physiological significance in planta.

DISCUSSION

HCS, catalyzing the covalent attachment of biotin, is ubiquitously represented in living organisms. In Arabidopsis, two *HCS* genes have been identified. However, our results establish that of the two *HCS* genes present in the Arabidopsis genome, only *HCS1* is essential and hence plays a major role in biotin-dependent carboxylase biotinylation. Moreover, we characterized an alternative splicing of the 5′-UTR of the *HCS1* mRNA. Interestingly, splicing of the 5′-UTR removes a small ORF (uORF24) situated upstream from the first AUG start codon. We showed that uORF24 could affect the initiation of *HCS1* translation and the choice between two in-frame AUG codons, targeting HCS1 either to the cytosol or to the chloroplasts. Altogether, these data enabled us to propose a model explaining the compartmentalization of HCS activity in planta with *HCS1* gene alone by an alternative splicing of its 5′-UTR.

Two Unequal Copies of *HCS* Genes in Arabidopsis

The two *HCS* genes identified in Arabidopsis, *HCS1* and *HCS2*, share 71% identity and probably result from an ancient event of duplication (Denis et al., 2002). However, the observation of their correspond-

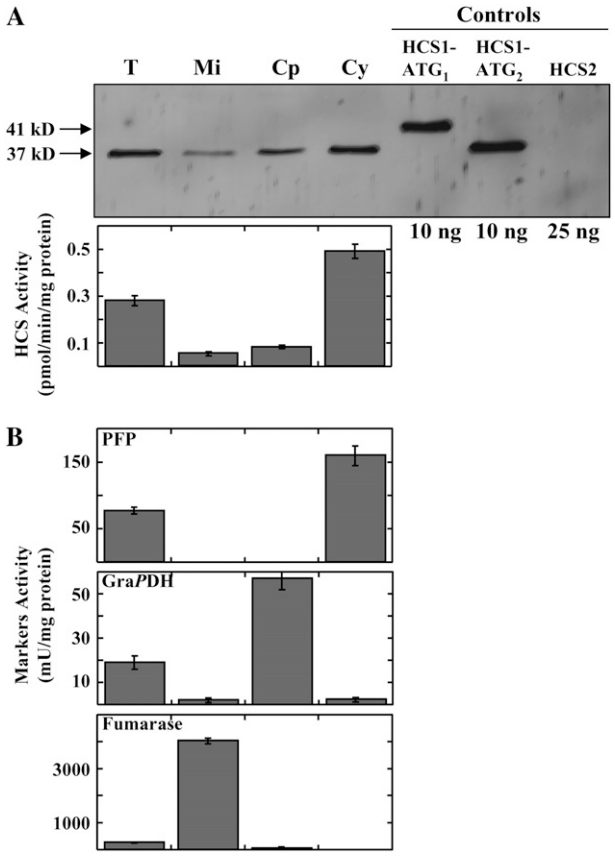

Figure 6. Evidence for multiple subcellular localizations of HCS1 in Arabidopsis. A, Soluble proteins (100 μg per lane) from a total leaf extract (T), purified mitochondria (Mi), purified chloroplasts (Cp), and a cytosolic-enriched fraction (Cy) were analyzed by western-blot analysis with affinity-purified polyclonal antibodies raised against recombinant HCS1 (Tissot et al., 1998). The same fractions were assayed for HCS specific activity. Pure recombinant HCS1-ATG_1 (HCS1 41-kD precursor form, 10 ng), HCS1-ATG_2 (HCS1 37-kD mature form, 10 ng), and HCS2 (37-kD gene product, 25 ng) proteins were run on the same gel as controls. B, Specific activities of cytosolic (pyrophosphate:Fru-6-P 1-phosphotransferase; PFP), chloroplast stroma (NADP-dependent glyceraldehyde-3-P dehydrogenase; GraPDH), and mitochondrial matrix (fumarase) markers were measured (Tissot et al., 1997) to analyze cross-contaminations between subfractions. Data are means ± SD of three replicates.

Table I. *Synthetic oligonucleotides used*

Primer Name	Primer Sequence	Annealing Temperature[a]
Genotyping of *hcs1* mutant		
Hcs1.for	5′-CTGCCTCAGGTTCGAAACTATTAGGAC-3′	
Hcs1.rev	5′-TAACACACAAAGGTAATCAACCAACC-3′	
LB3	5′-TAGCATCTGAATTTCATAACCAATCTCG-3′	
Isolation and genotyping of *hcs2* mutant		
Hcs2.Met	5′-CGTTATTGAACAGTTTCGTGGTCATGC-3′	
Hcs2.Stop	5′-CATCTGCGTTCACCAAAAGATGCTTC-3′	
Tag3	5′-CTGATACCAGACGTTGCCCGCATAA-3′	
Tag5	5′-CTACAAATTGCCTTTTCTTATCGACCATG-3′	
Exon7	5′-GGAGCTTTACTATAGGACATGGC-3′	
Real-time PCR		
Hcs2.Q5	5′-CCAGTTGGTTCAGTTTGTGTCTCTGATATACAAC-3′	60°C
Hcs2.Q3	5′-GGCACTACTCGACCATCTTCCATTTCTAAT-3′	60°C
Hcs1.Q5	5′-CCAGTTGGTTCAGTTTGTGTCACTGATATCCAGT-3′	64°C
Hcs1.Q3	5′-GGCACGACTCGACCATCTTCCATTTCTAGA-3′	64°C
Left minus	5′-GAACGAACTGCTTCCATTAAACTGTTGT-3′	60°C
Left plus	5′-GAACGAACTGCTTCCATTAAACTATAA-3′	60°C
Right	5′-AGCTCTCCTCTGCATCTGAGCATTGC-3′	60°C
Actin.5	5′-GTTTTGCTGGGGATGATGC-3′	55°C
Actin.3	5′-GGATTGAGCTTCATCGCC-3′	55°C
5′-RACE experiment		
Hcs1.E4	5′-CCATACATTCTTTGTTCTGC-3′	
BCCP2, ACC138, cloning and expression		
5′-bccp2	5′-AAATCTGAACATATGGCTAAAGTCTCTGG-3′	
3′-bccp2	5′-GCAGCTAAAGAGCTCCTTCTT-3′	
5′-acc	5′-AGTAAATATCATATGGATGTAGTCC-3′	
3′-acc	5′-TTATTTTGAGCTCAATCAAGATCAAGATTGGC-3′	
Mutagenesis		
ATG0.for	5′-CGAATAGCAGCAAGATCTTTGATTTGGCTAC-3′	
ATG0.rev	5′-GTAGCCAAATCAAAGATCTTGCTGCTATTCG-3′	
Cloning of *HCS1* cDNA variants		
RACE.KPN	5′-TTAAATTAAAGGTACCGCTCTCCTCTGCATC-3′	
STOP1.SAC	5′-AAAATCTTGAGCTCATATTTTTCTTCGTCGAAC-3′	
HCS1-GFP fusion cloning		
ATG1.XBA	5′-GATCTAGATGGAAGCAGTTCGTTCAAC-3′	
Hcs1s.XBA	5′-ACAGCTCTAGACTGCATCTGAGCATTG C-3′	
ATG2.XBA	5′-CAACCTTATCTAGATTTCATCTACTG-3′	
Hcs1un.XBA	5′-GTCTTCTAGATTAAAAATTGCAACTTTAAC-3′	
Hcs1.BAM	5′-CCCTTAAACTGGATCCCAGTGACAC-3′	

[a]The annealing temperature used for the real-time PCR is indicated.

ing mutants shows that they do not share equal responsibility for protein biotinylation. The *hcs1* mutant is lethal and, in contrast, the *hcs2* mutant is perfectly viable and does not present any obvious defect in biotinylation. As a result, they are not functionally redundant. This implies that only *HCS1* is probably responsible for carboxylase biotinylation and that *HCS2* makes little, if any, direct contribution to these reactions in vivo. Because biotin-dependent carboxylases are activated by the fixation of their cofactor and their apoforms are inactive, the lethality observed upon *HCS1* disruption is most probably associated with a defect of carboxylase activity. ACCases are catalyzing the first step of fatty acid synthesis in the plastids or of very-long-chain fatty acid elongation in the cytosol. Their activity alone is crucial for cell viability (Alban et al., 2000; Baud et al., 2004), and its defection is probably enough to explain the lethality observed upon *HCS1* disruption. HCS1 is able to biotinylate in vitro apocarboxylase substrates from various subcellular compartments (Tissot et al., 1998; Denis et al., 2002). In Arabidopsis, MCC-α, the biotinyl subunit of MCCase, is localized in the mitochondrion; ACC1, the homomeric ACCase isoform, is localized in the cytosol; and BCCP1 and BCCP2, the biotinyl subunits of heteromeric ACCase isoforms, are localized in the plastid (Alban et al., 2000). Our data offer a mechanism by which HCS1 can be targeted to cytosol and plastids, compartments where it could biotinylate its different substrates and where HCS activity had been detected (Tissot et al., 1997; Denis, 2002). Finally, the question arises whether HCS1 could also be targeted to mitochondria. Indeed, HCS activity also occurs in plant mitochondria (Tissot et al., 1997; this study). Furthermore, HCS1 does not present a canonical transit peptide sequence, indicative of a possible joint

plastid and mitochondrial targeting. Examples of dual targeting of a single translation product in chloroplasts and mitochondria through the utilization of a single ambiguous presequence have been described (Peeters and Small, 2001; Karniely and Pines, 2005). Western-blot analyses strongly suggest that in addition to the cytosol and chloroplasts, HCS1 is also targeted to mitochondria in Arabidopsis. However, despite a thorough survey of protoplasts expressing the HCS1-GFP constructs, we were unable to detect fluorescence in mitochondria. This may reflect a lack of sensitivity in the GFP assay; in case of an uneven dual distribution of a protein, its most abundant localization can impede the detection of the minor one (Duchene et al., 2005). It is also possible that the GFP promoter fusion missed essential cis-elements that aid its targeting to mitochondria but are not necessary for plastidic targeting (Christensen et al., 2005; Kabeya and Sato, 2005).

The *HCS2* gene does not seem to bear any fundamental function in carboxylase biotinylation in plants, reporting on *HCS1* gene, which is essential for plant viability, the whole responsibility of biotin-dependent carboxylase biotinylation within the cell. Is there a function for *HCS2*? The event of whole duplication of the Arabidopsis genome gives many examples of pairs of duplicate genes, and their relative functions and evolution have been documented. Many duplicated genes are retained and their redundancy might facilitate genetic robustness against null mutations (Gu et al., 2003). Unequal genetic redundancies, where the absence of a mutant phenotype in loss-of-function mutants of one gene contrasts with a strong phenotype in mutants of its homolog, have also been recently discussed (Briggs et al., 2006). Examples have been described in which genes do not act redundantly in vivo because of a difference of expression level or pattern. Such a scenario has been observed, for instance, for the proteasome subunit RPN1A and RPN1B: *RPN1A* loss-of-function results in embryo lethality, whereas *rpn1b* mutants are fully viable and resemble the wild type (Brukhin et al., 2005). The nondispensable allele *RPN1A* is expressed at much higher levels than *RPN1B*. This does not seem to be the case for *HCS1* and *HCS2* duplicated pair. Although *HCS2* is located in the pericentromeric region of chromosome 1, it is constitutively and ubiquitously expressed in Arabidopsis plants (Denis et al., 2002). However, none of the mRNA produced by *HCS2* gene expression was shown to encode an in vitro active HCS protein. Thus, one cannot exclude that *HCS2* could be an inactive pseudogene in Arabidopsis. This possibility would be consistent with the observations that the *HCS2* gene, unlike the *HCS1* gene, is characterized by a high level of nucleotide polymorphism inside ecotype Wassilewskija, indicating relatively weak functional constraint on the *HCS2* gene (Denis et al., 2002). This is also consistent with global sequence analyses showing that pericentromeres are remarkably dynamic, undergoing rapid changes in structure and sequence content (Hall et al., 2006). Another possibility is that *HCS2* could have a function as a noncoding RNA. Recent evidence points to a widespread role of these molecules in eukaryotic cells (Mattick and Makunin, 2006; Costa, 2007). Interestingly, in mice, *Makorin1-p1*, an expressed pseudogene, was shown to regulate the mRNA stability of its protein-coding homologous gene, *Makorin1* (Hirotsune et al., 2003). However, we showed that in the *hcs2* mutant, the *HCS1* mRNA level was unchanged. As a result, *HCS2* does not seem to have any direct function in *HCS1* mRNA stability. Finally, besides its classical role in carboxylase biotinylation, evidence is emerging that HCS in mammalian cell nuclei participates in the epigenetic control of chromatin structure and gene expression through biotinylation of histones (Narang et al., 2004; Zempleni, 2005). To date, these challenging fields of research remain unexplored in plants. Thus, one cannot exclude such functions for *HCS2* gene in Arabidopsis. This question clearly deserves future study.

A Control of HCS1 Translation Initiation by uORF24

We have identified a uORF within 5′-UTR of *HCS1* mRNA and showed that it could influence AUG choice and *HCS1* main ORF translation initiation. The uORFs are common features of eukaryotic genes, occurring in 10% to 25% of 5′ leader sequences (Crowe et al., 2006; Neafsey and Galagan, 2007). They have been generally found to decrease translational efficiency of the downstream coding sequence (Meijer and Thomas, 2003; Vilela and McCarthy, 2003). Indeed, in accordance with the scanning model of translation initiation (Kozak, 2002), uORFs interfere with translation of a downstream main ORF. They have been shown to negatively impact translational efficiency through a variety of means, including ribosome blocking by the encoded peptide, ribosome stalling at the uORF termination codon, and failure to reinitiate at the genic translation start site after disengaging from the uORF (Gaba et al., 2001). The reinitiation mechanism describes the ability of 40S subunits to continue to scan and initiate at a downstream main AUG codon after translating a small independent uORF. Our data show that the presence of uORF24 not only decreases the translation of downstream *HCS1* but also influences AUG choice. This makes it possible that uORF24 acts by inducing a reinitiation of translation after disengaging of the ribosome at its termination codon. In the presence of uORF24 within 5′-UTR (*HCS1.un* mRNA), ribosomes would initiate translation at the AUG_0 codon (more favorable to initiation than AUG_1; Pedersen and Nielsen, 1997). After translation of uORF24, the 40S subunit may hold on the mRNA, resume scanning, and reinitiate at a downstream AUG codon. However, reinitiation at AUG_1 would probably not be possible because it is too close (four nucleotides) from uORF24 termination (see Fig. 3) and would not give the 40S ribosomal subunit its required distance to reacquire Met-tRNAi and initiation factor eIF2 (Kozak, 1999, 2002). Possibly, after translation of uORF24, ribosomes could recover a suf-

ficient reinitiation competency only when they reach AUG_2. In the absence of uORF24 (*HCS1.s* mRNA), ribosomes initiate translation at AUG_1 according to the scanning model. As a result, the general translation initiation rules could explain the observed effect of uORF24 on *HCS1* translation initiation efficiency. Although our data are consistent with the above proposed model, further work is needed to fully address the mechanism of AUG selection governed by uORF24, particularly the precise ribosome behavior. Finally, *HCS1* gives an original example where a uORF has more than a simple effect on translation efficiency and can control the further targeting of the produced peptide.

Is Molecular Control of HCS Compartmentalization an Adaptation to Environmental Changes?

The occurrence of an alternative splicing of *HCS1* 5′-UTR is another original feature of *HCS1* translation initiation control by uORF24. Indeed, uORF24 inhibitory effect on AUG_1 utilization can be abrogated when it is spliced out. Another example of such control of a uORF action by its elimination through alternative splicing has been described in human *vigilin* mRNA (Rohwedel et al., 2003). In the case of *HCS1*, it is interesting to position this alternative splicing in the context of general metabolic regulations. As mentioned above, HCS1 is a key component of biotin-dependent metabolisms (fatty acid synthesis, amino acid catabolism). The central role of plant HCS in converting inactive apoenzymes into their active holoforms makes it a key enzyme in the maintenance of active plant metabolism. Thus, the relative biotinylation of a biotin-containing enzyme may be a crucial mechanism for regulating its activity. In support of this suggestion, we previously observed that the evolution of HCS activity during plant development paralleled with the activities of biotin-dependent carboxylases (Tissot et al., 1996). Our present results evidenced some fine regulations of HCS1 activity and targeting at the mRNA level. It is possible that metabolites can modulate these molecular mechanisms by direct interactions with *HCS1* mRNA. Bacteria and higher organisms can use cis-acting regulatory RNAs that function as direct receptors for intracellular metabolites (riboswitches) to regulate expression of their genes (Winkler, 2005; Thore et al., 2006). Riboswitches are UTRs of mRNA, which adopt alternate structures depending on the binding of specific metabolites. Interestingly, a recent study in *Neurospora crassa* showed that the expression of the *NMT1* gene (a known gene of the thiamine metabolism) was regulated at the level of pre-mRNA splicing by a riboswitch that bound thiamine pyrophosphate. Thiamine pyrophosphate binding on the riboswitch controls the alternative splicing of *NMT1* 5′-UTR, which in turn, by eluding or revealing small uORFs, controls the efficiency of initiation at the main ORF (Cheah et al., 2007). Our results and model, in light of these arising mechanisms of gene expression control, offer exciting prospects for the study of metabolic-related regulations and rapid variations of the cellular metabolism under developmental or stress conditions.

CONCLUSION

Control of gene expression by sequence elements in the mRNA 5′ leader is still not well understood, and new mechanisms of control continue to be uncovered. Our work describes a novel situation in which the presence or removal, by alternative splicing, of a uORF governs start codon selection in the main ORF, which in turn controls organelle versus cytosolic localization of a multi-targeted enzymatic gene product. This provides a possibility for fine molecular regulation and, beyond the specific issue of HCS protein, unveils the general complexity of plant metabolism compartmentalization.

MATERIALS AND METHODS

Media, Bacterial Strains, and Chemicals

D-[8,9-^{3}H]Biotin (33 Ci mmol^{-1}), [α-^{32}P]dCTP (3,000 Ci mmol^{-1}), and [^{35}S]L-Met (1,175 Ci mmol^{-1}) were purchased from GE Healthcare. Isopropylthio-β-D-galactoside was obtained from Bioprobe Systems. All other biochemicals were obtained from Sigma-Aldrich. The oligonucleotide primers utilized in this study are listed in Table I.

Temperature-sensitive *Escherichia coli birA215* mutant (strain BM4050) was generously provided by Dr. A.M. Campbell. Mutations in the birA gene affect the biotin ligase function of the BirA protein. The mutant had been lysogenized with the helper phage (λDE3) harboring a copy of the T7 RNA polymerase gene, using the λDE3 lysogenization kit from Novagen (Tissot et al., 1998). The resulting *E. coli* birA215 (DE3) was transformed by pET vectors encoding biotin-dependent carboxylases under the control of the T7 promoter. The recombinant carboxylases were then essentially expressed as their apo forms.

Plant Materials and Growth Conditions

A putative Arabidopsis (*Arabidopsis thaliana*) T-DNA insertion line for *HCS1* (SAIL_1277_E03; line *hcs1-1*) of the ecotype Columbia identified in the Syngenta Arabidopsis Insertion Library (Sessions et al., 2002) was obtained from the Arabidopsis Biological Resource Center. The Arabidopsis *hcs2* (EAG32 line) mutant of the ecotype Wassilewskija was obtained by screening of the T-DNA insertion line collection from the Station Génétique et d'Amélioration des Plantes (INRA, Versailles, France). Plants were grown in soil under greenhouse conditions (23°C with a 16-h photoperiod and a light intensity of 200 μmol photons m^{-2} s^{-1}) until harvested for analysis. For screening, seeds were surface sterilized and germinated on half-strength Arabidopsis medium solidified with agar (0.7%, w/v; Estelle and Somerville, 1987). After a cold treatment of 48 h at 4°C in the dark, the plates were transferred to a growth chamber and incubated at 24°C under a 16-h-light/8-h-dark regime. Selection of T-DNA-containing seeds was performed by germination on half-strength Arabidopsis medium supplemented with 50 mg L^{-1} kanamycin (*hcs1-2* and *hcs2* mutants) or by spraying seedlings (*hcs1-1* mutant) with 240 μg mL^{-1} glufosinate ammonium (BASTA). Arabidopsis (ecotype Columbia) cell suspension cultures were grown under continuous white light (40 μE m^{-2} s^{-1}) at 23°C with rotary agitation at 125 rpm in Gamborg's B5 medium supplemented with 1 μM 2-naphtalene acetic acid and 1.5% (w/v) Suc.

Isolation of T-DNA Insertion Line of *HCS2*

DNA pools of the Arabidopsis T-DNA insertion lines from the Versailles collection were screened for T-DNA insertion in the *HCS2* locus (At1g37150). Forward (hcs2.met) and reverse (hcs2.stop) primers from the coding sequence

of the *HCS2* locus were designed for PCR screening of the DNA pools by the combination of T-DNA left (Tag5) and right (Tag3) border-specific primers. PCR products were analyzed by southern hybridization of duplicate membranes to both the *HCS2* gene probe generated from the entire *HCS2* gene and the T-DNA probe. A positive PCR product was identified from megapool-16 and further amplified positively in Superpool-48 and in primary pool 189A by *HCS2* locus primer hcs2.stop and T-DNA primer Tag5. T-DNA insertion in the *HCS2* gene was confirmed by sequencing the resulting positive PCR fragment. The 48 lines from the primary pool 189A were further screened, and line 21 (EAG32) was identified for T-DNA insertion in the *HCS2* gene. Homozygous mutant plants were isolated from line 21 by PCR analysis using two sets of primers (exon7/hcs2.stop gene primers and Tag5 [T-DNA primer]/hcs2.stop) combined with kanamycin selection (resistance is conferred by the T-DNA). Homozygous mutant plants were confirmed by Southern-blot analysis using the *HCS2* gene probe generated by PCR amplification of the entire *HCS2* gene.

Plant DNA Isolation and Blotting

DNA was isolated from plant tissues by a standard method (Dellaporta et al., 1983). Blotting and hybridization were performed as described previously (Tissot et al., 1997).

Identification of *HCS1* Transcription Start Site

The transcription start site of *HCS1* was determined by 5′-RACE using Arabidopsis leaf cDNAs (Denis et al., 2002). Two sequential PCRs were performed with two pairs of nested adaptor primers and gene-specific primer in exon 4 of *hcs1* (Hcs1.E4). The resulting PCR products were cloned into pPCRscript (Stratagene) and sequenced.

Cloning of *HCS1* cDNA Splicing Variants

Poly(A) mRNAs from Arabidopsis rosette leaves were prepared using the Straight A's mRNA isolation system according to the manufacturer's instructions (Novagen), followed by a treatment with RNase-free DNase I. First-strand cDNA was synthesized from 250 ng of DNA-free mRNA in a final volume of 20 μL using oligo(dT)$_{20}$ primers (Thermoscript RT-PCR system; Life Technologies). PCR reaction was then conduced using 1-μL aliquots of the RT reaction and *HCS1*-specific primers in the presence of 1 unit of Pwo polymerase (Roche). *HCS1*-specific oligonucleotides (RACE.KPN/STOP1.SAC) were chosen according to *hcs1* cDNA and 5′-RACE sequences to amplify both full-length splicing variants. They introduced a *Kpn*I restriction site and a *Sac*I restriction site. After digestion with *Kpn*I and *Sac*I enzymes, RT-PCR products were cloned into pPCRscript digested by the same enzymes, yielding pPCRscript-HCS1.s and pPCRscript-HCS1.un constructs, respectively.

Real-Time PCR

Relative quantification experiments were done by real-time PCR using Rotor Gene system (Corbett Research) and SYBR Green Jump Start Taq Readymix (Sigma-Aldrich).

For each measurement, 1 μL of cDNA preparation was used as a template in 7.5 μL of Readymix with appropriate primers (used at a final concentration of 0.5 or 1 μM). Amplification and detection were performed using the following profile: 95°C/2 min followed by 45 cycles of 95°C/15 s, X°C/20 s, and 72°C/20 s. The annealing temperature (X°C) that is primer dependent is indicated in Table I. The specificity of the reaction was verified by melting curve analysis obtained by increasing the temperature from 72°C to 95°C.

Poly(A) mRNAs from different organs (leaves, stems, roots, flowers, siliques, and seeds) of Arabidopsis were prepared using Straight A's mRNA Isolation system (Novagen), followed by a treatment with RNase-free DNase I. First-strand cDNA was synthesized from 1 μg of DNA-free mRNA in a final volume of 20 μL using oligo(dT)$_{20}$ primers (Thermoscript RT-PCR system; Life Technologies) and used for real-time PCR analyses as described above. The relative amount of *HCS1* and *HCS2* cDNAs was determined using the PCR primers hcs2.Q.5, hcs2.Q.3, hcs1.Q.5, and hcs1.Q.3 (Denis et al., 2002; Table I). *HCS1* cDNA splicing variants were discriminated using Left Plus/Right and Left Minus/Right primers (Table I). Control reactions omitting RT were run for all samples to ensure that genomic DNA contamination did not contribute to the amplified products. Expression data were normalized to the constitutively expressed *ACTIN1* mRNA (Denis et al., 2002). The primers used for *ACTIN1*-derived cDNA amplification were actin.3 and actin.5 (Table I).

In Vitro Transcription/Translation Experiments

pPCRscript-HCS1.s and pPCRscript-HCS1.un, obtained by RT-PCR, encoding *HCS1* cDNA splice variants under the control of T7 promoter, and pPCRscript-HCS1.ATG$_0$m obtained by site-directed mutagenesis of the pPCRscript-HCS1.un construct were linearized by digestion with *Afl*III and transcribed with T7 RNA polymerase from mMessage mMachine kit (Ambion) in accordance with the instructions of the manufacturer. Capped *HCS1* mRNAs produced were then translated using a reticulocyte lysate from Ambion kit (Retic lysate IVT) and [^{35}S]Met in accordance with the instructions of the manufacturer. A control reaction with empty plasmid was performed under the same conditions. Radiolabeled proteins were separated by SDS-PAGE and analyzed by phosphorimaging analysis using a Typhoon 9400 scanner (GE Healthcare Europe).

GFP Fusion Targeting Analyses

A pUC18 plasmid expressing the modified version mGFP4 of GFP under the control of the cauliflower mosaic virus 35S promoter (p35S:GFP; Haseloff et al., 1997) was used for transient expression experiments in Arabidopsis protoplasts. cDNA sequences comprising the 5′-UTR splice variants and region encoding the first 142 residues of *HCS1* ORF were fused upstream and in frame with *mGFP4* sequence. These regions were PCR amplified using *pfu* DNA polymerase, pPCRscript constructs as templates, and the specific flanking primers listed in Table I. The PCR products were digested with *Xba*I and *Bam*HI and inserted between the *Xba*I and *Bam*HI sites of pGFP to give plasmids p35S:HCS1.un-GFP and p35S:HCS1.s-GFP. p35S:HCS1.ATG$_0$m-GFP was obtained by site-directed mutagenesis of p35S:HCS1.un-GFP plasmid. Control *35S:HCS1-GFP* fusion constructs lacking the 5′-UTR region of *HCS1* cDNAs and starting at the ATG$_1$ (p35S:HCS1.ATG$_1$-GFP) or the ATG$_2$ (p35S:HCS1.ATG$_2$-GFP) codon were also performed, using specific primers (Table I). GFP chimera bearing the transit peptide sequences of the small subunit of Rubisco from Arabidopsis (55 residues, *ATS1A* gene, GenBank accession no. X13611) and dihydropterin pyrophosphokinase/dihydropteroate synthase from pea (*Pisum sativum*; 28 residues; Rébeillé et al., 1997) were used as controls for the targeting of GFP to plastids and mitochondria, respectively. Transient transformation of Arabidopsis protoplasts prepared from a 4-d-old cell suspension culture was achieved using 40 μg of plasmid construct by the polyethylene glycol method, essentially as described (Abel and Theologis, 1994). Transformed cells were incubated at 23°C for 36 h and analyzed by epifluorescence microscopy using a Zeiss Axioplan2 fluorescence microscope, and images were captured with a digital CCD camera (Hamamatsu). The filter sets used were Zeiss filter set 13, 488013-0000 (exciter BP 470/20, beamsplitter FT 493, emitter BP 505–530) and Zeiss filter set 15, 488015-0000 (exciter BP 546/12, beamsplitter FT 580, emitter LP 590), for GFP and chlorophyll fluorescence, respectively.

Mutagenesis of *HCS1* 5′-UTR

Plasmids pPCRscript-HCS1.ATG$_0$m and p35S:HCS1.ATG$_0$m-GFP were obtained using the QuikChange mutagenesis protocol (Stratagene) and plasmids pPCRscript-HCS1.un and p35S:HCS1.un-GFP, respectively. Oligonucleotides were designed to replace the initiation codon (ATG$_0$) of the uORF of *HCS1* 5′-UTR region by an ATC codon and to modify the restriction enzyme digestion profile for identification of mutants. Positive mutants were sequenced to ensure that no other mutations were present.

Cloning, Expression, and Purification of Recombinant apo-BCCP1, apo-BCCP2, apo-MCC220, and apo-ACC138

Recombinant Arabidopsis apo-BCCP1 (the biotin carboxyl carrier subunit of chloroplastic ACCase; At5g16390) devoid of the chloroplast transit peptide and apo-MCC220 (the C-terminal 220 amino acids of methylcrotonyl-CoA carboxylase α-subunit, comprising the biotinylation domain; At1g03090) were produced as described previously (Tissot et al., 1998; Denis et al., 2002).

The pET-28b+-BCCP2 and pET-28b+-ACC138 plasmids encoding the Arabidopsis biotinyl proteins BCCP2 (a second isoform of the biotin carboxyl carrier subunit of plastid ACCase; At5g15530) devoid of the plastid transit peptide and ACC138 (the 138 amino acids biotinylation domain of cytosolic ACCase isoform 1, comprising amino acids 609–746 of the protein sequence; At1g36160) were constructed by means of PCR using Arabidopsis leaf cDNAs.

Primers used for amplifications were synthesized in accordance with the published cDNA or gene sequences and to the comparison of biotinylation domains of various known biotin-dependent carboxylases (Table I; Samols et al., 1988; Cronan, 1990; Yanai et al., 1995; Thelen et al., 2001). They introduced a *Nde*I restriction site in 5′ and a *Sac*I restriction site in 3′. After digestion with *Nde*I and *Sac*I, the PCR fragments were subcloned into pET28b+ vector (Novagen) digested with the same enzymes. The *E. coli* birA215 (DE3) strain transformed with plasmid constructs was grown and induced at 37°C in Luria-Bertani medium supplemented with kanamycin (50 μg mL^{-1}). When A_{600} reached 0.6, 0.5 mM isopropylthio-β-D-galactoside was added and growth was continued at 28°C for 3 to 4 h. Cells were collected by centrifugation and resuspended in buffer A containing Tris-HCl 25 mM, pH 7.5, 0.3 M NaCl, and 10 mM imidazole. Cells were then disrupted by sonication with a Vibra-Cell disrupter (100 pulses every 3 s on power setting 5). The soluble protein extracts were separated from the cell debris by centrifugation at 40,000*g* for 15 min. Finally, recombinant proteins produced were purified by metal-chelate column chromatography (Ni-NTA agarose, Qiagen) according to the manufacturer's instructions.

Activity Measurements

Samples of Arabidopsis plants were harvested, ground in liquid nitrogen with a mortar and pestle, and homogenized in 1 volume of chilled buffer B composed of 20 mM Tris-HCl, pH 7.5, 1 mM EDTA, 1 mM dithiothreitol, 5 mM ε-aminocaproic acid, 1 mM benzamidine-HCl, and 1 mM phenylmethylsulfonyl fluoride. After 15 min centrifugation (40,000*g*), the supernatants were subjected to ammonium sulfate precipitation with crystalline ammonium sulfate to 80% saturation. The resulting precipitates were collected by centrifugation and resuspended in a minimum volume of buffer B. The suspensions were desalted onto PD10 columns (Pharmacia) and used for further analysis. HCS activity in the protein extracts was measured according to the protocol described previously (Tissot et al., 1996) using purified BCCP1, BCCP2, ACC138, and MCC220 as the apocarboxylase substrates. Biotin-dependant carboxylase activities were measured as the incorporation of radioactivity from $NaH^{14}CO_3$ into acid-stable products (Baldet et al., 1993). Acetyl-CoA and methylcrotonoyl-CoA were used as acceptor substrates.

Western-Blot Analyses

Total soluble proteins from Arabidopsis leaves were extracted as described above. Proteins were resolved by SDS-PAGE and electroblotted to nitrocellulose membrane. Biotin-containing polypeptides were detected with a system analogous to western blotting using streptavidin conjugated with horseradish peroxidase (Baldet et al., 1992). The presence of streptavidin-biotin complexes was analyzed by chemiluminescence. For the purpose of HCS1 immunodetection, chloroplasts and mitochondria from Arabidopsis leaves were isolated and purified with Percoll gradients as described previously (Pinon et al., 2005). Soluble proteins were obtained from the purified organelles after osmotic lysis and centrifugation (Pinon et al., 2005). A cytosolic-enriched fraction was prepared from Arabidopsis protoplasts by using the procedure described by Pinon et al. (2005). After protein separation by SDS-PAGE and electrotransfer to nitrocellulose membrane, the blots were probed by using HCS1 polyclonal antibodies produced in rabbits (Tissot et al., 1998), horseradish peroxidase-conjugated anti-rabbit IgGs, and detection was achieved by chemifluorescence by using the ECL Plus Western Blotting Detection Reagents and a Typhoon 9400 scanner (GE Healthcare Europe). Pure recombinant HCS1-ATG$_1$, HCS1-ATG$_2$, and HCS2 proteins, produced as described previously (Tissot et al., 1998; Denis, 2002), were run on the same gel to serve as size controls and for verifying the specificity of the antibody.

Sequence data from this article can be found in the GenBank/EMBL data libraries under accession numbers *ACC1*, *At1g36160*; *ACTIN1*, *At2g37620*; *BCCP1*, *At5g16390*; *BCCP2*, *At5g15530*; *HCS1*, *At2g25710*; *HCS2*, *At1g37150*; *MCC-α*, *At1g03090*.

Supplemental Data

The following materials are available in the online version of this article.

Supplemental Figure S1. Analysis of a second independent T-DNA insertion allele of Arabidopsis *HCS1* (FLAG_486E08; *hcs1-2* line).

ACKNOWLEDGMENTS

We thank the Arabidopsis Biological Resource Center (The Ohio State University, Columbus) and the Arabidopsis Resource Centre for Genomics (INRA, Versailles, France) for providing seeds of the T-DNA-inserted *hcs1* Arabidopsis mutants. We thank David Bouchez and Fabienne Granier from the Station Génétique et d'Amélioration des Plantes (INRA, Versailles, France) for providing access to the collection of T-DNA insertion mutants and enabling us to isolate the T-DNA inserted *hcs2* Arabidopsis mutant. We also thank Laetitia Brunel for technical assistance, François Parcy for his help with genetic crossing studies, and Michel Matringe and Stéphane Ravanel for critical reading and helpful comments on the manuscript.

Received October 23, 2007; accepted December 13, 2007; published December 21, 2007.

LITERATURE CITED

Abel S, Theologis A (1994) Transient transformation of *Arabidopsis* leaf protoplasts: a versatile experimental system to study gene expression. Plant J **5:** 421–427

Alban C, Job D, Douce R (2000) Biotin metabolism in plants. Annu Rev Plant Physiol Plant Mol Biol **51:** 17–47

Arabidopsis Genome Initiative (2000) Analysis of the genome sequence of the flowering plant *Arabidopsis thaliana*. Nature **408:** 796–815

Baldet P, Alban C, Axiotis S, Douce R (1992) Characterization of biotin and 3-methylcrotonyl-coenzyme A carboxylase in higher plant mitochondria. Plant Physiol **99:** 450–455

Baldet P, Alban C, Axiotis S, Douce R (1993) Localization of free and bound biotin in cells from green pea leaves. Arch Biochem Biophys **303:** 67–73

Baud S, Bellec Y, Miquel M, Bellini C, Caboche M, Lepiniec L, Faure JD, Rochat C (2004) gurke and pasticcino3 mutants affected in embryo development are impaired in acetyl-CoA carboxylase. EMBO Rep **5:** 515–520

Bouchez D, Camilleri C, Caboche M (1993) A binary vector based on Basta resistance for in planta transformation of *Arabidopsis thaliana*. C R Acad Sci Ser III Sci Vie **316:** 1188–1193

Briggs GC, Osmont KS, Shindo C, Sibout R, Hardtke CS (2006) Unequal genetic redundancies in *Arabidopsis*: a neglected phenomenon? Trends Plant Sci **11:** 492–498

Brukhin V, Gheyselinck J, Gagliardini V, Genschik P, Grossniklaus U (2005) The RPN1 subunit of the 26S proteasome in *Arabidopsis* is essential for embryogenesis. Plant Cell **17:** 2723–2737

Cheah MT, Wachter A, Sudarsan N, Breaker RR (2007) Control of alternative RNA splicing and gene expression by eukaryotic riboswitches. Nature **447:** 497–500

Christensen AC, Lyznik A, Mohammed S, Elowsky CG, Elo A, Yule R, Mackenzie SA (2005) Dual-domain, dual-targeting organellar protein presequences in *Arabidopsis* can use non-AUG start codons. Plant Cell **17:** 2805–2816

Costa FF (2007) Non-coding RNAs: lost in translation? Gene **386:** 1–10

Cronan JE Jr (1990) Biotination of proteins in vivo. A post translational modification to label, purify and study proteins. J Biol Chem **265:** 10327–10333

Crowe ML, Wang XQ, Rothnagel JA (2006) Evidence for conservation and selection of upstream open reading frames suggests probable encoding of bioactive peptides. BMC Genomics **7:** 16

Dellaporta SL, Wood J, Hicks JBA (1983) A plant DNA minipreparation: version II. Plant Mol Biol Rep **1:** 19–21

Denis L (2002) Protein biotinylation in *Arabidopsis thaliana*: molecular and functional characterizations of *HCS1* and *HCS2* genes. PhD thesis. University of Grenoble, Grenoble, France

Denis L, Grossemy M, Douce R, Alban C (2002) Molecular characterization of a second copy of holocarboxylase synthetase gene (hcs2) in *Arabidopsis thaliana*. J Biol Chem **277:** 10435–10444

Duchene AM, Giritch A, Hoffmann B, Cognat V, Lancelin D, Peeters NM, Zaepfel M, Marechal-Drouard L, Small ID (2005) Dual targeting is the rule for organellar aminoacyl-tRNA synthetases in *Arabidopsis thaliana*. Proc Natl Acad Sci USA **102:** 16484–16489

Estelle MA, Somerville CR (1987) Auxin-resistant mutants of *Arabidopsis thaliana* with an altered morphology. Mol Gen Genet **206:** 200–206

Gaba A, Wang Z, Krishnamoorthy T, Hinnebusch AG, Sachs MS (2001) Physical evidence for distinct mechanisms of translational control by upstream open reading frames. EMBO J **20:** 6453–6463

Gu Z, Steinmetz LM, Gu X, Scharfe C, Davis RW, Li WH (2003) Role of duplicate genes in genetic robustness against null mutations. Nature **421:** 63–66

Hall AE, Kettler GC, Preuss D (2006) Dynamic evolution at pericentromeres. Genome Res **16:** 355–364

Hanfrey C, Franceschetti M, Mayer MJ, Illingworth C, Elliott K, Collier M, Thompson B, Perry B, Michael AJ (2003) Translational regulation of the plant S-adenosylmethionine decarboxylase. Biochem Soc Trans **31:** 424–427

Haseloff J, Siemering KR, Prasher DC, Hodge S (1997) Removal of a cryptic intron and subcellular localization of green fluorescent protein are required to mark transgenic *Arabidopsis* plants brightly. Proc Natl Acad Sci USA **94:** 2122–2127

Hirotsune S, Yoshida N, Chen A, Garrett L, Sugiyama F, Takahashi S, Yagami K, Wynshaw-Boris A, Yoshiki A (2003) An expressed pseudogene regulates the messenger-RNA stability of its homologous coding gene. Nature **423:** 91–96

Kabeya Y, Sato N (2005) Unique translation initiation at the second AUG codon determines mitochondrial localization of the phage-type RNA polymerases in the moss *Physcomitrella patens*. Plant Physiol **138:** 369–382

Karniely S, Pines O (2005) Single translation—dual destination: mechanisms of dual protein targeting in eukaryotes. EMBO Rep **6:** 420–425

Knowles JR (1989) The mechanism of biotin dependent enzymes. Annu Rev Biochem **58:** 195–221

Kozak M (1999) Initiation of translation in prokaryotes and eukaryotes. Gene **234:** 187–208

Kozak M (2002) Pushing the limits of the scanning mechanism for initiation of translation. Gene **299:** 1–34

Lunn JE (2007) Compartmentation in plant metabolism. J Exp Bot **58:** 35–47

Mattick JS, Makunin IV (2006) Non-coding RNA. Hum Mol Genet **15 Spec No 1:** R17–R29

McCarthy JE (1998) Posttranscriptional control of gene expression in yeast. Microbiol Mol Biol Rev **62:** 1492–1553

Meijer HA, Thomas AA (2002) Control of eukaryotic protein synthesis by upstream open reading frames in the 5′-untranslated region of an mRNA. Biochem J **367:** 1–11

Meijer HA, Thomas AA (2003) Ribosomes stalling on uORF1 in the xenopus Cx41 5′ UTR inhibit downstream translation initiation. Nucleic Acids Res **31:** 3174–3184

Morris DR, Geballe AP (2000) Upstream open reading frames as regulators of mRNA translation. Mol Cell Biol **20:** 8635–8642

Narang MA, Dumas R, Ayer LM, Gravel RA (2004) Reduced histone biotinylation in multiple carboxylase deficiency patients: a nuclear role for holocarboxylase synthetase. Hum Mol Genet **13:** 15–23

Neafsey DE, Galagan JE (2007) Dual modes of natural selection on upstream open reading frames. Mol Biol Evol **24:** 1744–1751

Nikolau BJ, Ohlrogge JB, Wurtele ES (2003) Plant biotin-containing carboxylases. Arch Biochem Biophys **414:** 211–222

Pedersen AG, Nielsen H (1997) Neural network prediction of translation initiation sites in eukaryotes: perspectives for EST and genome analysis. Proc Int Conf Intell Syst Mol Biol **5:** 226–233

Peeters N, Small I (2001) Dual targeting to mitochondria and chloroplasts. Biochim Biophys Acta **1541:** 54–63

Pinon V, Ravanel S, Douce R, Alban C (2005) Biotin synthesis in plants. The first committed step of the pathway is catalyzed by a cytosolic 7-keto-8-aminopelargonic acid synthase. Plant Physiol **139:** 1666–1676

Rébeillé F, Macherel D, Mouillon JM, Garin J, Douce R (1997) Folate biosynthesis in higher plants: purification and molecular cloning of a bifunctional 6-hydroxymethyl-7,8-dihydropterin pyrophosphokinase/7,8-dihydropteroate synthase localized in mitochondria. EMBO J **16:** 947–957

Rohwedel J, Kugler S, Engebrecht T, Purschke W, Muller PK, Kruse C (2003) Evidence for posttranscriptional regulation of the multi K homology domain protein vigilin by a small peptide encoded in the 5′ leader sequence. Cell Mol Life Sci **60:** 1705–1715

Samols D, Thornton CG, Murtif VL, Kumar GK, Haase FC, Wood HG (1988) Evolutionary conservation among biotin enzymes. J Biol Chem **263:** 6461–6464

Sessions A, Burke E, Presting G, Aux G, McElver J, Patton D, Dietrich B, Ho P, Bacwaden J, Ko C, et al (2002) A high-throughput *Arabidopsis* reverse genetics system. Plant Cell **14:** 2985–2994

Thelen JJ, Mekhedov S, Ohlrogge JB (2001) Brassicaceae express multiple isoforms of biotin carboxyl carrier protein in tissue-specific manner. Plant Physiol **125:** 2016–2028

Thore S, Leibundgut M, Ban N (2006) Structure of the eukaryotic thiamine pyrophosphate riboswitch with its regulatory ligand. Science **312:** 1208–1211

Tissot G, Douce R, Alban C (1997) Evidence for multiple forms of biotin holocarboxylase synthetase in pea (Pisum sativum) and in *Arabidopsis thaliana*: subcellular fractionation studies and isolation of a cDNA clone. Biochem J **323:** 179–188

Tissot G, Job D, Douce R, Alban C (1996) Protein biotinylation in higher plants: characterization of biotin holocarboxylase synthetase activity from pea (*Pisum sativum*) leaves. Biochem J **314:** 391–395

Tissot G, Pepin R, Job D, Douce R, Alban C (1998) Purification and properties of the chloroplastic form of biotin holocarboxylase synthetase from *Arabidopsis thaliana* overexpressed in *Escherichia coli*. Eur J Biochem **258:** 586–596

Vattem KM, Wek RC (2004) Reinitiation involving upstream ORFs regulates ATF4 mRNA translation in mammalian cells. Proc Natl Acad Sci USA **101:** 11269–11274

Vilela C, McCarthy JE (2003) Regulation of fungal gene expression via short open reading frames in the mRNA 5′untranslated region. Mol Microbiol **49:** 859–867

Winkler WC (2005) Riboswitches and the role of noncoding RNAs in bacterial metabolic control. Curr Opin Chem Biol **9:** 594–602

Yanai Y, Kawasaki T, Shimada H, Wurtele ES, Nikolau BJ, Ichikawa N (1995) Genomic organization of 251 kDa acetyl-CoA carboxylase genes in *Arabidopsis*: tandem gene duplication has made two differentially expressed isozymes. Plant Cell Physiol **36:** 779–787

Zempleni J (2005) Uptake, localization, and noncarboxylase roles of biotin. Annu Rev Nutr **25:** 175–196